2008 International Symposium on Nonlinear Theory and its Applications
NOLTA'08, Budapest, Hungary, September 7-10, 2008

Long-Range Dependence of Long-Term Continuous Intracranial Electroencephalograms for Detection and Prediction of Epileptic Seizures

Béla Weiss†, Zsuzsanna Vágó†, Ronald Tetzlaff‡ and Tamás Roska†

† Faculty of Information Technology, Péter Pázmány Catholic University
Budapest, Hungary
‡ Faculty of Electrical Engineering and Information Technology, Dresden University of Technology
Dresden, Germany
Email: weiss@itk.ppke.hu, vago@itk.ppke.hu, Ronald.Tetzlaff@TU-Dresden.de, roska@itk.ppke.hu

Abstract– Long-range dependence of long-term continuous intracranial electroencephalograms (*IEEG*) of three patients suffering from different types of epilepsy has been assessed by estimation of the Hurst exponent (*H*). Sensitivity of the estimation approach to different artifacts has been evaluated. A drop of *H* has occurred during all seizures. Gradual changes of *H* have been observed in the preictal and postictal periods. Based on these findings a seizure detection/prediction method has been developed.

1. Introduction

Epilepsy is the second most common neurological disorder, affects 1% of the world's population. For 25% of the patients no sufficient treatment is currently available. Novel diagnostic and therapeutic methods based on detection and prediction of epileptic seizures could improve the quality of live of these people [1].

Using short-term *IEEG* recordings we have shown that long-range dependence of brain electrical activity can be applied for detection of epileptic seizures [2], [3]. These results were confirmed by Osorio and Frei [4]. Our recent work revealed that fractal spectra of long-term *IEEG* show distinct changes in the preictal state of different types of human epilepsy [5]. In this study we attempt to confirm these results by estimation of *H* and to propose a seizure detection/prediction algorithm.

2. Data and Methods

2.1. Database

Long-term continuous *IEEG* data recorded during presurgical monitoring procedure were provided for this study by the following three institutes: Department of Epileptology, University of Bonn, Germany (*BEC*); National Institute of Neurosurgery, Budapest, Hungary (*NIN*); National Institute of Psychiatry and Neurology, Budapest, Hungary (*NIPN*).

Recording from *BEC* contained 10 clinical seizures of a patient suffering from mesial temporal lobe epilepsy (*MTLE*). The 5d 17h 41m long data were sampled at f_s=200 Hz using depth (two 1x10) and strip (four 1x4, and two 1x6) electrodes. *NIN* provided a 22h 33m long recording that contained four seizures from a patient suffering from frontal lobe epilepsy (*FLE*). These data were recorded by grid (right frontal convexity, 6x8 contacts; interhemispherial double sided with 2x2x5 contacts) and strip (two interhemispherial, 1x8 contacts; one cortical above right central and parietal convexity with 1x8 contacts) electrodes at f_s=500 Hz. The 2d 19h 51m long recording from *NIPN* contained 3 seizures of a patient suffering from *MTLE.* The sampling rate was f_s=256 Hz. Data were recorded by bilateral depth foramen ovale (*FO*) electrodes with four contacts.

All recordings were provided in raw format, without any filtering, and artifact removal.

2.2. Methods

The stochastic process *X(t)* with continuous parameter *t* is self-similar with self-similarity parameter *H* if the distribution of the rescaled process $c^{-H}X(ct)$ is the same as the distribution of *X(t)*, where $c>0$ is arbitrary. *H* is called the Hurst parameter or the Hurst exponent. When $0<H<0.5$, an increase in the process is more probably followed by a decrease and vice-versa, the process has short-range dependence. If $H=0.5$, observations of the process are uncorrelated. When $1>H>0.5$, an increase in the process is more probably followed by an increase and a decrease is more probably followed by a decrease, the process has long-range dependence [6], [7].

We have implemented the rescaled adjusted range or R/S statistics based method [7], [8] for the estimation of *H*. Let *X(i)* be a discrete time series. The partial sum process is denoted by *Y(n)*,

$$Y(n)=\sum_{i=1}^{n} X(i), \qquad n\in\mathbb{N}, \qquad Y(0)=0. \tag{1}$$

The sample variance of the process *X* is

$$S^2(n)=(1/n)\sum_{i=1}^{n} X(i)^2-(1/n)^2 Y(n)^2, \tag{2}$$

and the adjusted range is given by

$$R(n)=\max_{0\le i\le n}\Delta(i)-\min_{0\le i\le n}\Delta(i), \tag{3}$$

where

$$\Delta(i) = Y(i) - \frac{i}{n} Y(n). \quad (4)$$

The R/S statistics or the rescaled adjusted range is defined by

$$\frac{R}{S}(n) := \frac{R(n)}{S(n)}. \quad (5)$$

In [7] it was proven that for self-similar processes the expected value of *R/S (n)* is proportional to n^H, i.e.

$$E[R/S(n)] \sim C_H n^H, \quad (6)$$

as $n \to \infty$, where C_H is a positive constant and H is the self-similarity parameter of the process. Using this power law relationship the Hurst exponent can be estimated by:

$$H \sim \log(E[R/S(n)])/\log(n). \quad (7)$$

For a more convenient discussion the Hurst exponent and its estimate will be denoted by the same symbol H in this paper.

To estimate H, the N sample point long data segments were subdivided into K blocks. Blocks of length N/K corresponded to duration of 1 or 2 seconds. For each lag n, $R(k_i,n)/S(k_i,n)$ was computed, starting at points $k_i=iN/K+1$, $i=1, 2, \ldots, K$. Overlapping of blocks was avoided, the upper boundary i.e. the high cut-off point (*hcp*) of n was limited to N/K. This way we got K different estimates of $R(n)/S(n)$ for each value of lag n. By plotting $\log[R(k_i,n)/S(k_i,n)]$ versus $\log n$ we got the so-called pox plot for the R/S statistic. The parameter H can be estimated by fitting a line to the points in this plot, and it is equal to the slope of this line. Due to the transient zone at the low end of the plot we set a low cut-off point (*lcp*) as well. The low cut-off point was usually ~25% of N/K. Thus, we used only values of n that lie between the lower and higher cut-off points to estimate H. For a detailed description of this approach see [7], [8].

Before estimation no preprocessing was applied, raw data were used to minimize the computational cost and to reveal the sensitivity of the estimation method to artifacts.

3. Results

Fig. 1 compares the estimated H values for ictal (seizure) and interictal (between two seizures) data segments. These results suggest lower values of H during seizures.

The R/S based approach is valid only for stationary data. Due to the non-stationarity of *IEEG* signals, short (2s-90s) overlapping (*ol*) and non-overlapping data segments were tested to estimate H. These were considered stationary. Choosing an appropriate segment length (*sl*) is a trade-off (Fig. 2). For a better estimation we need more sample points. On the other hand, using longer segments we are unable to detect short perturbations and this can also cause longer estimation and detection delays what we would like to minimize during the real-time seizure detection prcedure. Drop of H

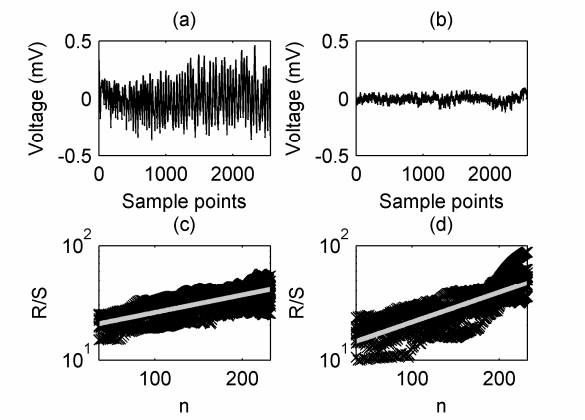

Fig. 1. Patient from *NIPN*, contact FO3. (a) 10s long ictal segment. (b) 10s long interictal segment, awake state. (c) Pox plot of (a), H = 0.5045. (d) Pox plot of (b), H = 0.8615. Settings: K = 10, *lcp* = 64, *hcp* = 250.

can be observed after the seizure onset time, during the ictal state as it was predicted by Fig. 1. Furthermore, gradual decrease of H can be observed in the 150s long preictal period before the seizure.

Sensitivity of the estimation method to different artifacts should be analyzed, since misinterpretation of the results can lead to false detections and predictions of the seizures. Moreover, automatic rejection of some artifacts during online, real-time application could be difficult due to a high computational cost or impossible, since in some cases this task still requires a human expert. Fig. 3 depicts data segments containing electrocardiogram (*ECG*) and 50Hz power line noise. The estimated H values of these signals are lower than H of data segments of interest presented in Fig. 1. This way, faulty electrodes contaminated with these artifacts could be excluded from analyses. However, if the *ECG* artifact occurs suddenly in one contact, it can produce a drop of H of similar extent as the drop during seizures. Common mode artifacts can be rejected using a bipolar montage (see Fig. 4 a-c). In this

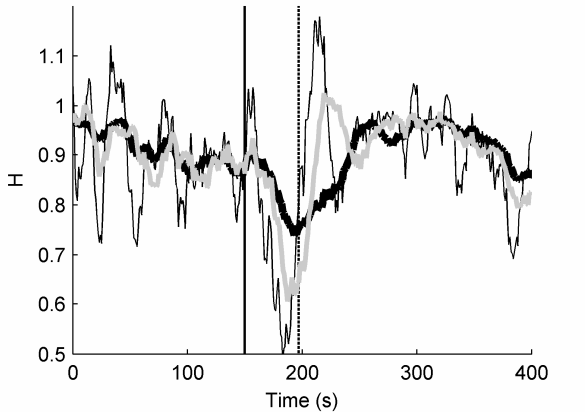

Fig. 2. Patient from *NIN*, contact IHJ10, first seizure. Thin black curve – *sl* = 10s, *ol* = 9s. Gray curve – *sl* = 30s, *ol* = 29s. Thick black curve – *sl* = 60s, *ol* = 59s. Common estimation parameters: *sl/K* = 1s, *lcp* = 100, *hcp* = 450. Vertical solid line – seizure onset time provided by *NIN*. Vertical dashed line – end of the seizure determined by *NIN*.

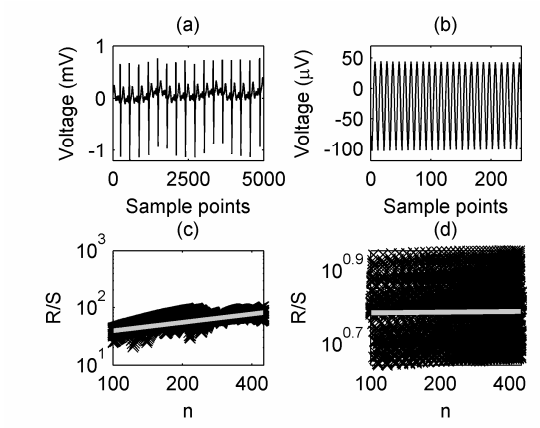

Fig. 3. Patient from *NIN*. (a) 10s long *ECG* segment. (b) 0.5s long segment recorded by faulty electrode contact. (c) Pox plot of (a), H = 0.4833. (d) Pox plot of 10s long segment that contains (b), H = 0.0058. Settings for estimation of H: K = 10, *lcp* = 100, *hcp* = 450.

case *IEEG* of adjacent contacts containing the same artifacts are subtracted from each other. Jumps of H denoted by vertical lines in Fig. 4 (a) and (b) disappear in (c).

To reduce the delay presented in Fig. 2, *sl* = 3s long non-overlapping data segments were used in Fig. 4. Moving average using sliding windows of different lengths was applied to the estimated H values to perform trend analysis. The moving average of the $X(i)$ discrete time series with $2q+1$, q = 1, 2, … long sliding window can be defined as:

$$Y(i)=\frac{1}{2q+1}\sum_{j=i-q}^{i+q}X(j). \tag{8}$$

The black curve in part (d) of Fig. 4 depicts average H of eight bipolar channels (IHJ1-IHJ2, IHJ2-IHJ3, IHJ4-IHJ5, IHJ6-IHJ7, IHB14-IHB15, GR5-GR6, GR6-GR7, CS7-CS8) selected by visual inspection of *IEEG* by clinicians from *NIN*. This way, the signal to noise ratio of H can be improved (compare c and d parts of the figure). Four drops of H can be observed during the 22h long recording of the patient suffering from *FLE*. These drops occurred immediately after the onsets of the seizures

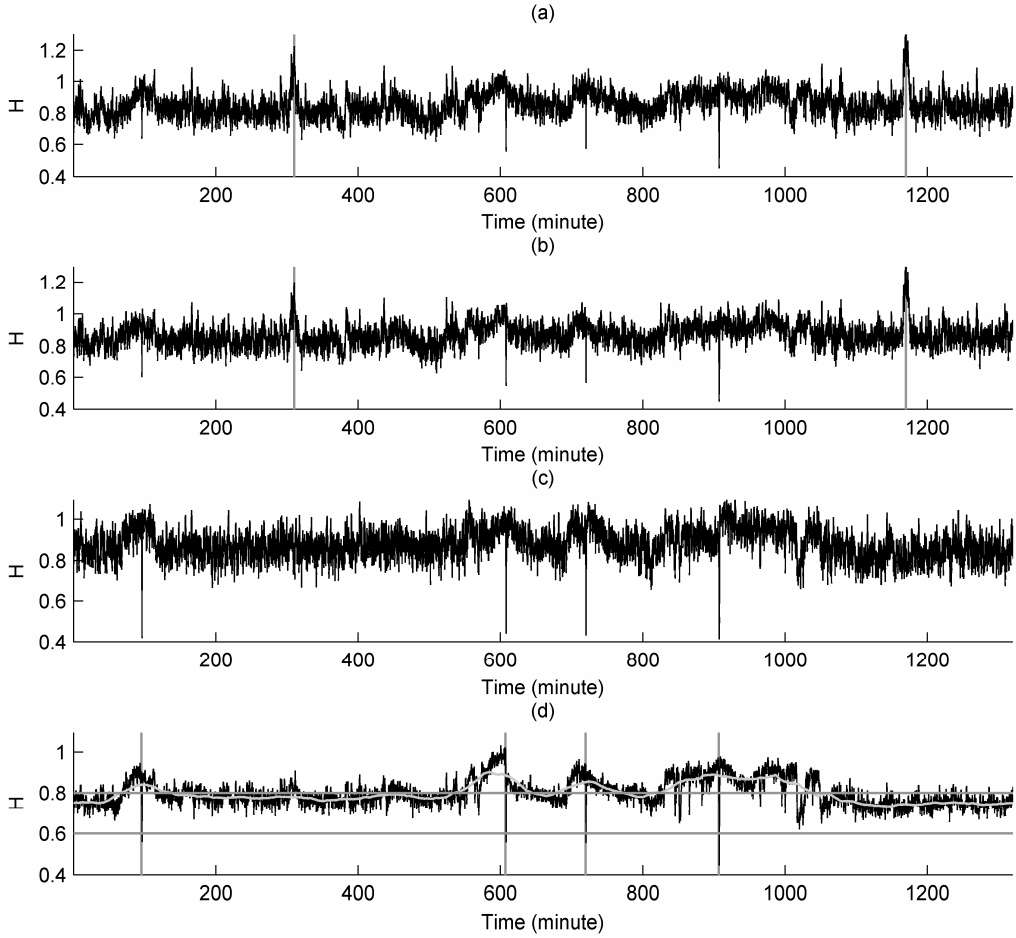

Fig. 4. Patient from *NIN*, 22h long recording, 4 seizures. (a) H of IHJ4 contact, q = 5. Vertical lines – jumps of H due to artifacts. (b) H of IHJ5 contact, q = 5. Vertical lines – jumps of H due to artifacts. (c) H of IHJ4-IHJ5 bipolar channel, q = 5. (d) Black curve – average H of 8 bipolar channels, q = 5. Gray curve – average H of 8 bipolar channels, q = 600. Vertical lines – seizure onset times provided by *NIN*. Horizontal lines - applied detection (H_{dt} = *0.6*) and prediction (H_{pt} = *0.8*) thresholds. (a) – (d) Common estimation settings: *sl* = 3s, K = 3, *lcp* = 100, *hcp* = 450.

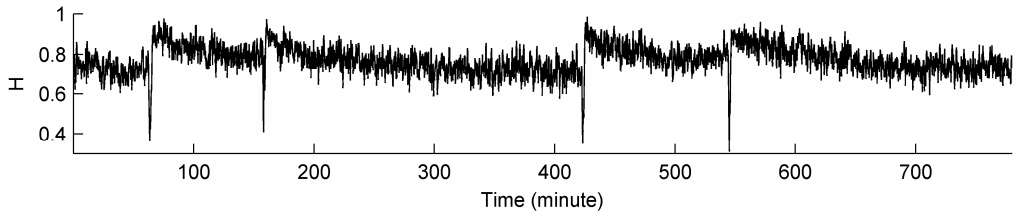

Fig. 5. Patient from *BEC*, 13h long recording, 4 seizures, *H* of the TL5 electrode contact placed into seizure generating left hippocampus. Estimation settings: sl = 3s, K = 3, lcp = 50, hcp = 199, q = 5.

denoted by the vertical lines. Before each drop there is a gradual increase. This long-term trend could not be observed using only the short-term recording in Fig. 2. Jumps of *H* appear as a rebound effect after the drops. Jumps are followed by gradual decrease in all four instances. Slower dynamics are emphasized by the gray curve which stands for the average *H* of the same eight bipolar channels but using a 1 hour long moving average window. This curve exceeds the applied prediction threshold (H_{pt} = *0.8*) 30 minutes and 9 seconds before the onset time of the first seizure. The first intersection of the black curve with the H_{dt} = *0.6* detection threshold appears 25 seconds after the onset of the seizure. Prediction intervals and detection delays for the other three seizures can be found in Table I. All seizures could be anticipated with a mean prediction interval of 59 m 28 s (Standard Deviation *SD = 28m 53s*) and detected with mean detection delay of 24.75s (*SD = 0.9574s*) without false positive alarms. Thus, with these particular settings we could achieve ideal results considering sensitivity (number of predicted or detected seizures divided by number of all seizures) and specificity (number of false positive prediction or detection alarms divided by total interictal time) measures for forecasting and detection as well.

TABLE I
PREDICTION AND DETECTION RESULTS FOR PATIENT FROM NIN

Seizure number	1	2	3	4
Detection delay	25s	24s	24s	26s
Prediction interval	30m 9s	72m 33s	41m 42s	93m 28s

Drop of *H* can also be observed during four seizures of the patient provided by *BEC* (Fig. 5). While in *FLE* we observed gradual increase of *H* before the seizures, in *MTLE* the opposite trend i.e. a gradual decrease is noticeable in the preictal states. Similar results were found for all seizures of the other patient (provided by *NIPN*) suffering from *MTLE*. The prediction method introduced for *FLE* should be modified in this case.

4. Conclusion

Long-range dependence of long-term continuous *IEEG* provides useful information about the dynamics of epileptic seizures. Drop of *H* has been observed during all 17 seizures, regardless the type of epilepsy. This phenomenon can allow detection of seizures. In the preictal states epilepsy type dependent trend has been found. This finding could imply different seizure generation mechanisms and propose different models and prediction approaches for seizures in *FLE* and *MTLE*. Statistical validation of the observed phenomena and verification of the goodness of the developed detection/prediction algorithm by determining sensitivity/specificity measures should be carried out using a large database.

Acknowledgments

The authors would like to thank *BEC*, *NIN* and *NIPN* for the provided recordings. This research was supported by the Hungarian Molecular Biology and Info-bionics in Medical Research Grant: RET - 05/2004, OMFB – 01426/2004.

References

[1] F. Mormann, C. E. Elger, K. Lehnertz,“ Seizure anticipation: from algorithms to clinical practice,” *Current Opinion in Neurology*, vol. 19, pp. 187-193, 2006.
[2] B. Weiss, Z. Vágó, T. Roska, „Epileptic seizure prediction and detection based on Hurst exponent estimation,” presented at the IXth Workshop on Neurobiology of Epilepsy, Langkawi, Malaysia, 2007, to be published in *Epilepsia*.
[3] B. Weiss, Z. Vágó, R. Tetzlaff, T. Roska, “Long-range dependence of epileptic seizures,“ presented at the 3rd International Workshop on Epileptic Seizure Prediction, Freiburg, Germany, 2007.
[4] I. Osorio, M. Frei, “Hurst parameter estimation for epileptic seizure detection,” *Communication in Information and Systems*, vol. 7, no. 2, pp. 167-176, 2007.
[5] B. Weiss, B. Hegedűs, Z. Vágó, T. Roska, “Fractal spectra of intracranial electroencephalograms in different types of epilepsy,” in *19th International Conference BIOSIGNAL*, 2008, ID 115, pp. 1-5.
[6] J. Beran, *Statistics for Long-Memory Processes*. Boca Raton, London, New York, Washington, DC., Chapman & Hall, 1994.
[7] B. B. Mandelbrot, M. S. Taqqu, “Robust R/S analysis of long-term serial correlation,” *Bulletin of the International Statistical Institute*. vol. 48, book 2, pp. 69-104, 1979.
[8] Murrad S. Taqqu. R/S Method [Online]. Available: http://math.bu.edu/people/murad/methods/rs/rs.web.ps